



**The Abdus Salam
International Centre for Theoretical Physics**



2145-17

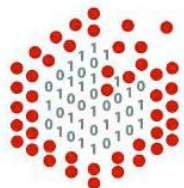
Spring College on Computational Nanoscience

17 - 28 May 2010

Theory of GW

Layla MARTIN SAMOS
CNR IOM DEMOCRITOS
Trieste
Italy

Charged $N+1$ / $N-1$ excitations and the GW approximation



DEMOCRITOS

DEmocritos MOdeling Center for
Research In aTOMIC Simulation

Overview

- Brief overview on the theoretical basis and main concepts
- GW in practice
- Example: amorphous SiO₂

The Many-Body Problem

N-electrons interacting through the Coulomb potential:

$$H = \sum_{i=1}^N T(x_i) + \sum_{i \neq j=1}^N V(x_i, x_j) + \sum_{\alpha} \sum_{i=1}^N V_{ext}(x_i, R_{\alpha})$$

Field operators representation:

$$\hat{H} = \int d^3x \hat{\psi}^{\dagger}(x) T(x) \hat{\psi}(x) + \frac{1}{2} \int \int d^3x d^3x' \hat{\psi}^{\dagger}(x) \hat{\psi}^{\dagger}(x') V(x, x') \hat{\psi}(x') \hat{\psi}(x) + \sum_{\alpha} \int d^3x \hat{\psi}^{\dagger}(x) V_{ext}(x, R_{\alpha}) \hat{\psi}(x)$$

Many-Body Problem in terms of Green functions

The Feynman rules for finding the contribution of n th order perturbation theory are simpler.

The use of Green functions imply the loss of detailed information although they still contain:

- 1.) The expectation value of any single-particle operator in the ground state
- 2.) The ground state energy
- 3.) The excitation spectrum.

One-particle Green Function

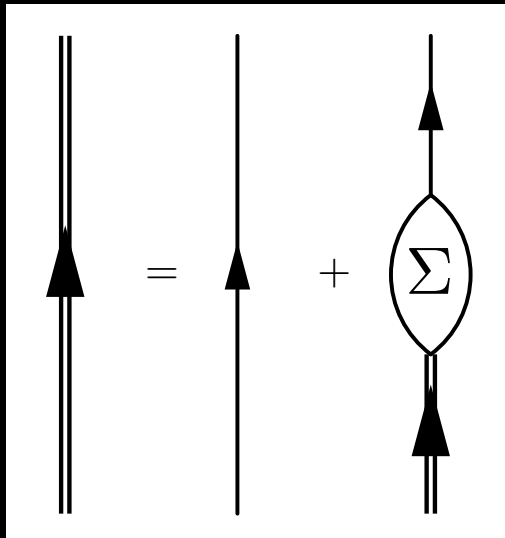
$$iG_{\alpha\beta}(xt, x't') = \frac{\langle \Psi_0 | T[\hat{\psi}_{H\alpha}(xt) \hat{\psi}_{H\beta}^\dagger(x't')] | \Psi_0 \rangle}{\langle \Psi_0 | \Psi_0 \rangle}$$

spin index

Heisenberg operators

$$\hat{\psi}_{H\alpha}(xt) = e^{i\hat{H}t/\hbar} \hat{\psi}_\alpha(x) e^{-i\hat{H}t/\hbar}$$

Dyson's Equations



Solving a Dyson equation corresponds to summing an infinite class of diagrams!

$$G_{\alpha\beta}(12) = G_{\alpha\beta}^0(12) + \int d3d4 G_{\alpha\lambda}^0(13) \Sigma_{\lambda\mu}(34) G_{\mu\beta}(42)$$

The Quasi-Particle concept

Suppose an interaction invariant under translation and a system spatially uniform.

The quantities 1, 2, ... , depends only on coordinate differences thus a four dimensional Fourier transform can be defined.

Dyson Equation in Fourier space:

$$G(k) = G^0(k) + G^0(k)\Sigma(k)G(k)$$

$$G(k) = \frac{1}{[G^0(k)]^{-1} - \Sigma(k)}$$



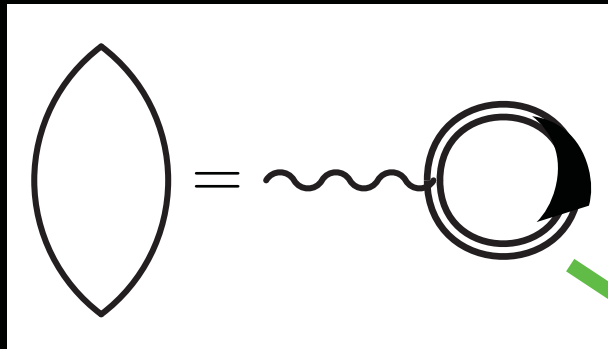
$$G(k, \omega) = \frac{1}{\omega - \epsilon_k^0 - \Sigma(k, \omega)}$$

H^{QP}

- $H^{\text{QP}} \rightarrow N+1/N-1$ electronic excitations

Approximations to the self-energy

Hartree

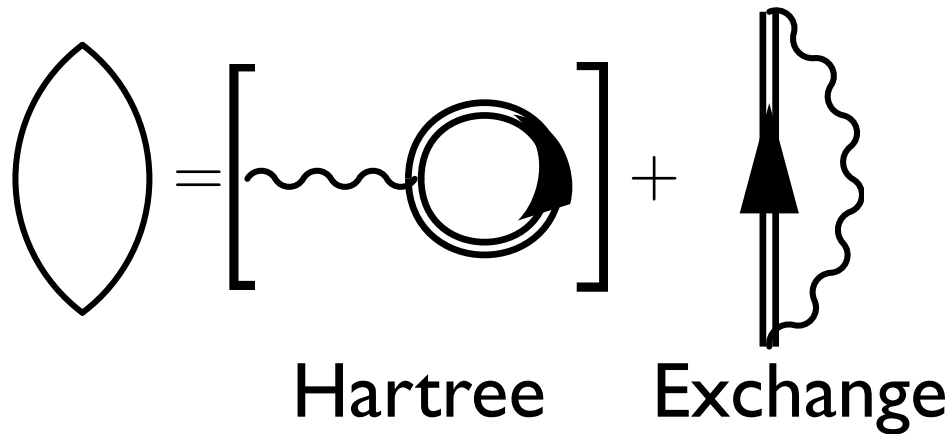


Single-particle equation, solvable,
shifts non-interacting particle
energies.

$$F[\tilde{n}(r)] \equiv T_s[\tilde{n}(r)] + \frac{1}{2} \int \frac{\tilde{n}(r)\tilde{n}(r')}{|r-r'|} drdr' + E_{xc}[\tilde{n}(r)]$$

” Σ ”

Hartree-Fock



$$\Sigma \equiv \Sigma_x(12) = iv(12)G(12)$$

Creation of an electron/hole at the vacuum level that propagates filling a mean **bare-coulomb-interacting** electronic sea

Beyond

Converge with the **bare Coulomb** potential is very long and difficult ~ Multiple SCF Configuration Interaction ...

UNAFFORDABLE but for small molecules

Expansion with a **screened Coulomb** potential:

Hedin Equations or *GW*

GWT

Set of five equations to be solved self-consistently

$$G(12) = G^0(12) + \int d3d4 G^0(13) \Sigma(34) G(42)$$

$$P(12) = -i \int G(23) G(42) \Gamma(341) d(34)$$

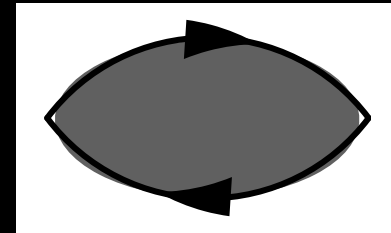
$$W(12) = v(12) + \int W(13) P(34) v(42) d(34)$$

$$\Sigma(12) = i \int W(1^+3) G(14) \Gamma(423) d(34)$$

$$\Gamma(123) = \delta(12)\delta(13) + \int \frac{\delta\Sigma(12)}{\delta G(45)} G(46) G(75) \Gamma(673) d4567$$

Vertex corrections, or the filled bubble

Response of the system
when an **interacting**
electron-hole pair is created



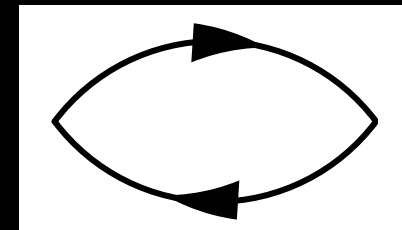
$$P(1, 2) = -i \int G(23)G(42)\Gamma(341)d(34)$$

Assuming:

$$\Gamma(123) = \delta(12)\delta(13)$$

RPA, or the empty bubble

Response of the system
when a **non-interacting**
electron-hole pair is created



$$P(1, 2) = -iG(12)G(21)$$

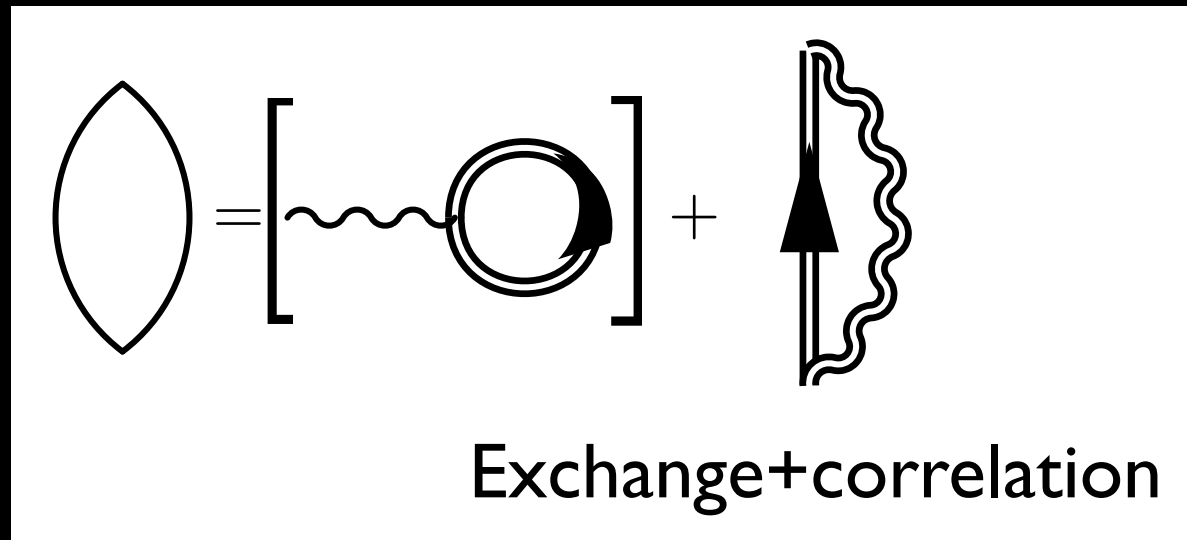
Hedin Equations within GW approximation

Self-consistency

$$G(12) = G^0(12) + \int d3d4 G^0(13) \Sigma(34) G(42)$$

$$\begin{aligned} P(12) &= -iG(12)G(21) \\ W(12) &= v(12) + \int W(13)P(34)v(42)d(34) \\ \Sigma(12) &= iW(1^+2)G(12) \end{aligned}$$

Creation of an electron/hole at the vacuum level
that propagates filling a polarized electronic sea



**GW ~ Hartree-Fock with a
“dressed” self-energy**

#The dress (W) is non-local, energy dependent



L. Reining & CO lessons (<http://etsf.polytechnique.fr>, training)



A. L. Fetter and J. D. Walecka, *Quantum Theory of Many-Particle Systems*, Dover (New York, 2003).



L. Hedin and S. Lundqvist, *Solid State Phys.* **29**, 1 (1969)

Why do we need GW?

- 1.) Hartree-Fock does not include correlations.
- 2.) Multiple scf Configuration Interaction contains all, computational too much demanding, affordable only for small molecules.
- 3.) DFT -> needs an ad-hoc build of “Universal Functionals”, available functionals fail for the band energy gap, for charged defect formation energies, etc.

GW is not “La vie en rose”

A part, deep theoretical questions on diagrams taken into account, there **still do not exist an univocal agreement on its practical implementation and its range of use.**

GW as it is, from Hedin’s equation, is still computationally **unaffordable for “realistic” systems.**

GW objects are:

- Non-local (functions of $|r-r'|, |r''-r'''|, GG'q$)
- Energy dependent
- Calculation of the self-energy needs or a real time integration or an energy convolution (thin grid due to poles).
- Usually needs sums on unoccupied states (slow convergence)

$$\langle nk | \Sigma^x | n'k \rangle = -\frac{1}{N\Omega} \sum_{vq} \sum_G \theta(\mu - \epsilon_{vk-q}) M_{vk-q, nk}^*(G) v_q^C(G) M_{vk-q, n'k}(G)$$

$$\langle nk | \Sigma_c(\omega) | n'k \rangle = -\frac{1}{N\Omega} \sum_{n''q} \sum_{GG'} M_{n''k-q, nk}^*(G) M_{n''k-q, n'k}(G') \times$$

$$\frac{-1}{2\pi i} \int d\omega' \frac{W_{GG'}^p(q; \omega') e^{-i\delta\omega'}}{\omega + \omega' - \epsilon_{n''k-q} - i\eta \text{sign}(\mu - \epsilon_{n''k-q})}$$

Main approximations

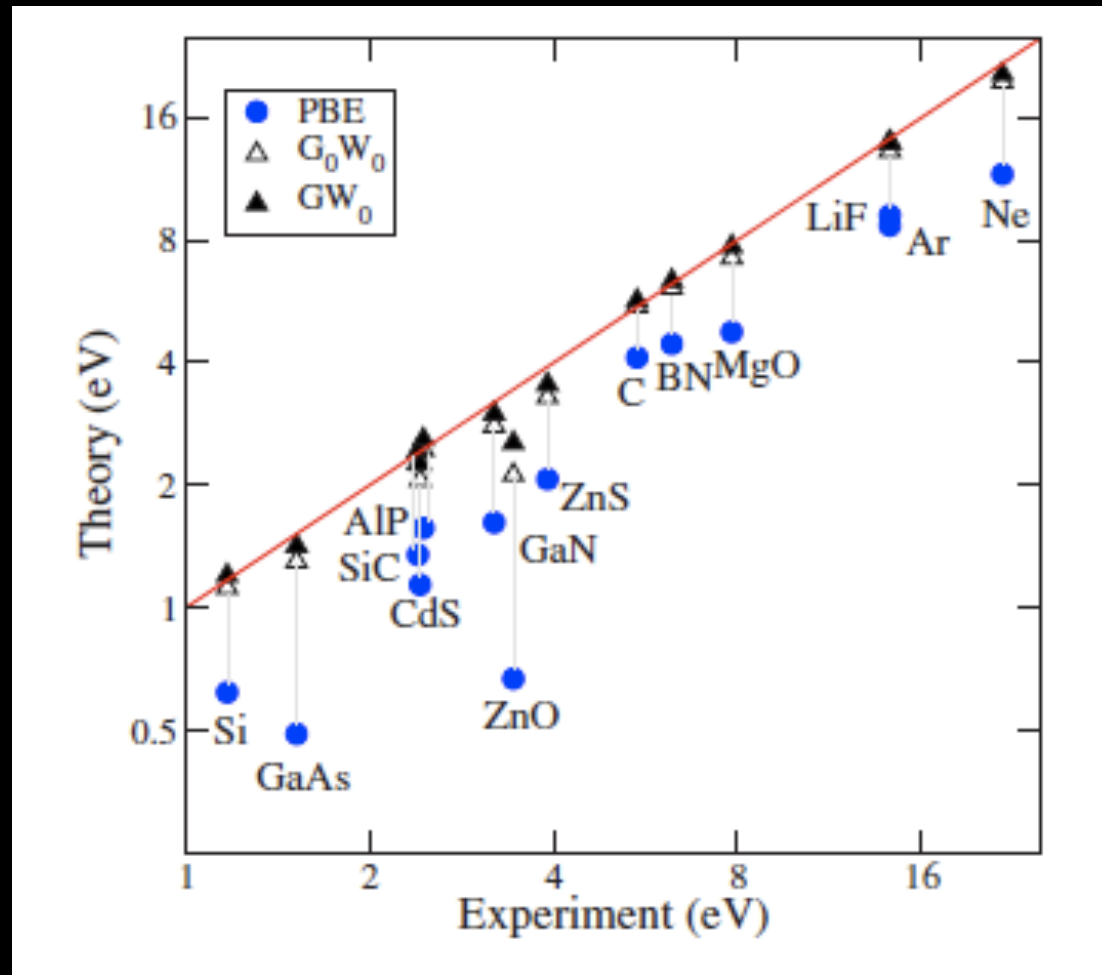
- Pseudo-potentials
- No Self-Consistency! -> dependency on the starting point.
- Diagonal approximation -> starting point wave functions
- Not real-time or real energy convolution.

Not enough benchmarks

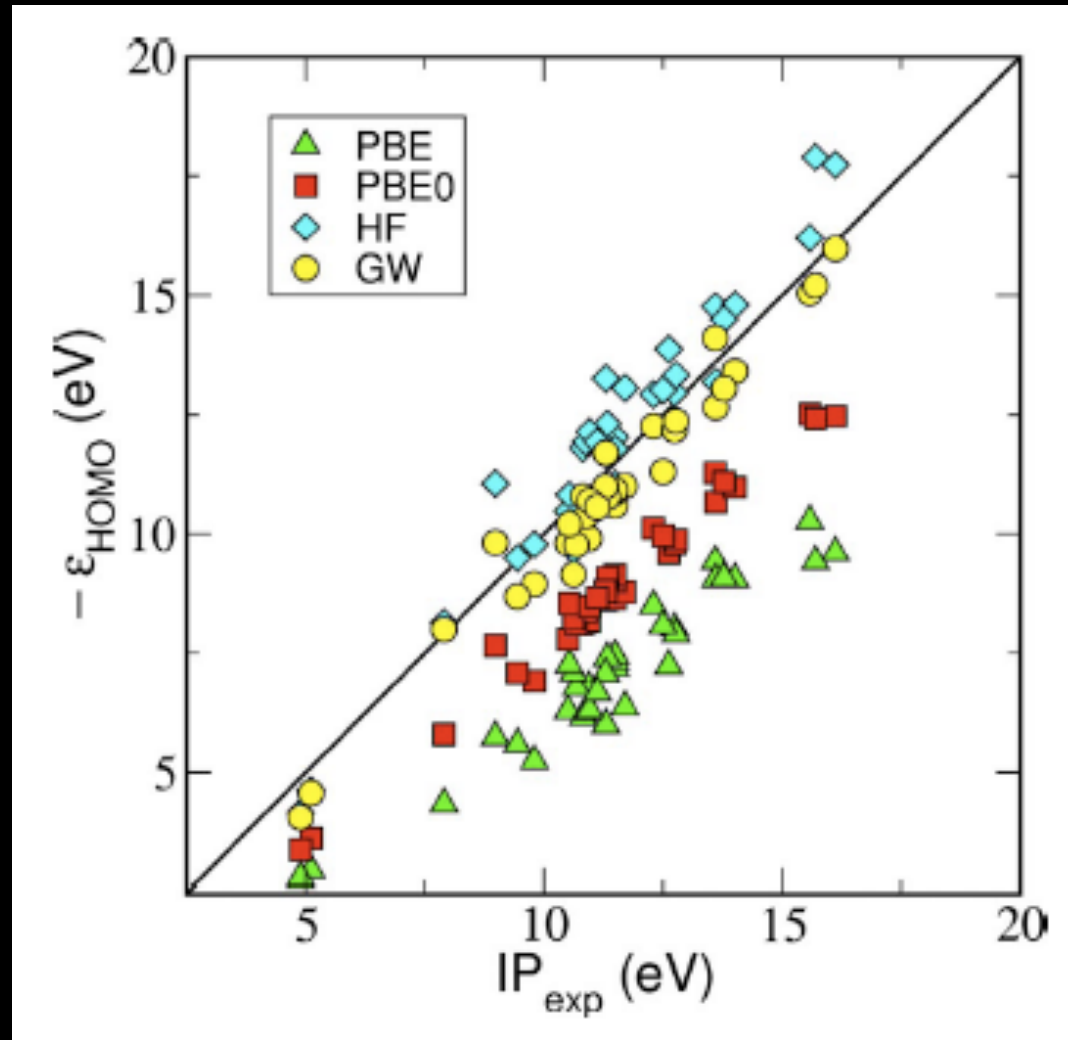
Main “hidden” approximations

- LDA/GGA pseudo-potentials, core-valence interaction never consistent!
- How long wavelength limit (and neighborhood) is treated.

Great success for bulk semiconductors/insulators



Some interesting results for molecules



Example

Amorphous SiO₂

Prototypical strong glass, forming tetrahedral SiO₄
disordered networks

Used in many fields : microelectronic industry (for metal-oxide-semiconductor devices), optical fiber technologies and nano-imprint lithography, etc.

Disorder?

- Thermal (crystals and glasses)
 - Bond length and bond angle variations (vibrations)Equilibrium defects, etc

- Frozen-in (glasses)

Degree of freedom frozen-in at the glass transition

- Bond length and bond angle distributions
- Medium range “structures”
- Long range -> homogeneous system (Liquid like)

Disorder?

- Thermal (crystals and glasses)

- Bond length and bond angle distributions
- Equilibrium defects, etc

Small disorder



- Frozen-in (glasses)

Degree of freedom frozen-in at the glass transition

- Bond length and bond angle distributions
- Medium range “structures”
- Long range -> homogeneous system (Liquid like)

Disorder?

- Thermal (crystals and glasses)

- Bond length and bond angles
- Equilibrium defects, etc

Small disorder



- Frozen-in (glasses)

Degree of freedom frozen-in at the glass transition

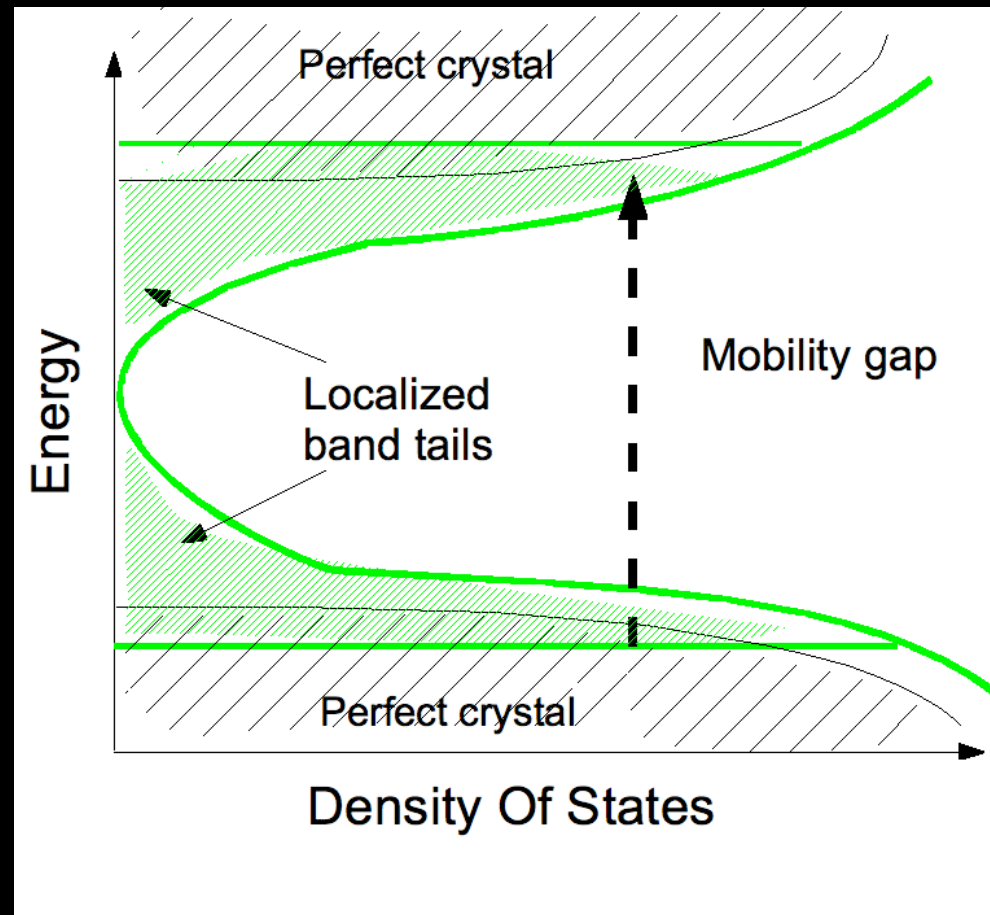
- Bond length and bond angles
- Medium range "structures"

Strong disorder

- Long range -> homogeneous system (Liquid like)



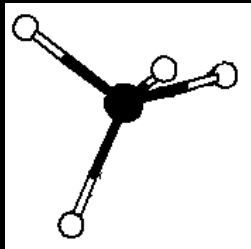
Disorder in semiconductors and insulators



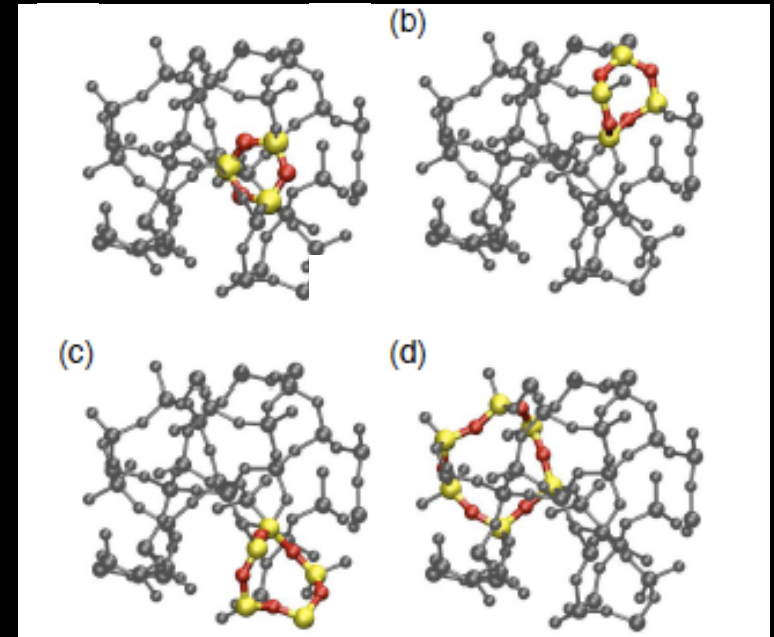
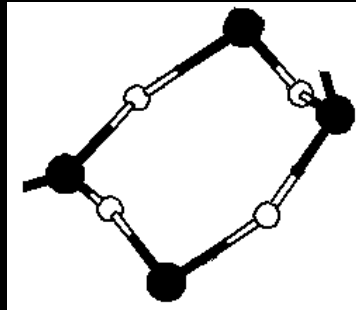
Observed in a-Si:H

Connected network of SiO_4 tetrahedra

Short range:
tetrahedron



Medium range: rings



Long range: Periodic/homogeneous

In tetrahedral crystal systems the band gap increases with the density

a-SiO₂ (dens. ~2.2 g/cm³), quartz (dens. ~2.6 g/cm³),
cristobalite (dens. ~2.2 g/cm³)

In tetrahedral crystal systems the band gap increases with the density

a-SiO₂ (dens. ~2.2 g/cm³), quartz (dens. ~2.6 g/cm³),
cristobalite (dens. ~2.2 g/cm³)

Experimental findings

No band tails near fundamental/mobility gap are found
Gap's between Quartz and silica -> no marked differences

Mobility gap $\sim 8.9(1)-9.62(2)-11.53(3)$

Absorption edge $\sim 8.54(4) - 8.95(5)$

1) onset of photo-conductivity: Z.A. Weinberg et al, Phys Rev B 19, 3107 (1979)

2) X ray photoemission: V. J. Nithianandam and S. E. Schnatterly, Phys. Rev. B 38, 5547 (1988)

3) R. Evrard and A. N. Trukhin, Phys. Rev. B 25, 4102 (1982)

4) optical absorption: K. Saito and A. J. Ikushima, Phys Rev B 62 8584 (2000)

5) photoinjection threshold: T. H. DiStefano and D. E. Eastman, Solid State Commun 9 2259 (1971)

Theoretical results

- Parametrized Hamiltonians on model systems: small disorder degree closes the mobility gap while strong disorder open it (1).
- DFT: no localized tails in conduction, slight localization at valence. α -SiO₂ gap slightly smaller than quartz (2).
- “GW”: cristobalite slightly smaller gap than quartz (3-4).

1) F. Fazileh et al, PRB 73 035124 (2006)

2) J. Sarnthein, A. Pasquarello and R. Car PRL 74 4682 (1995)

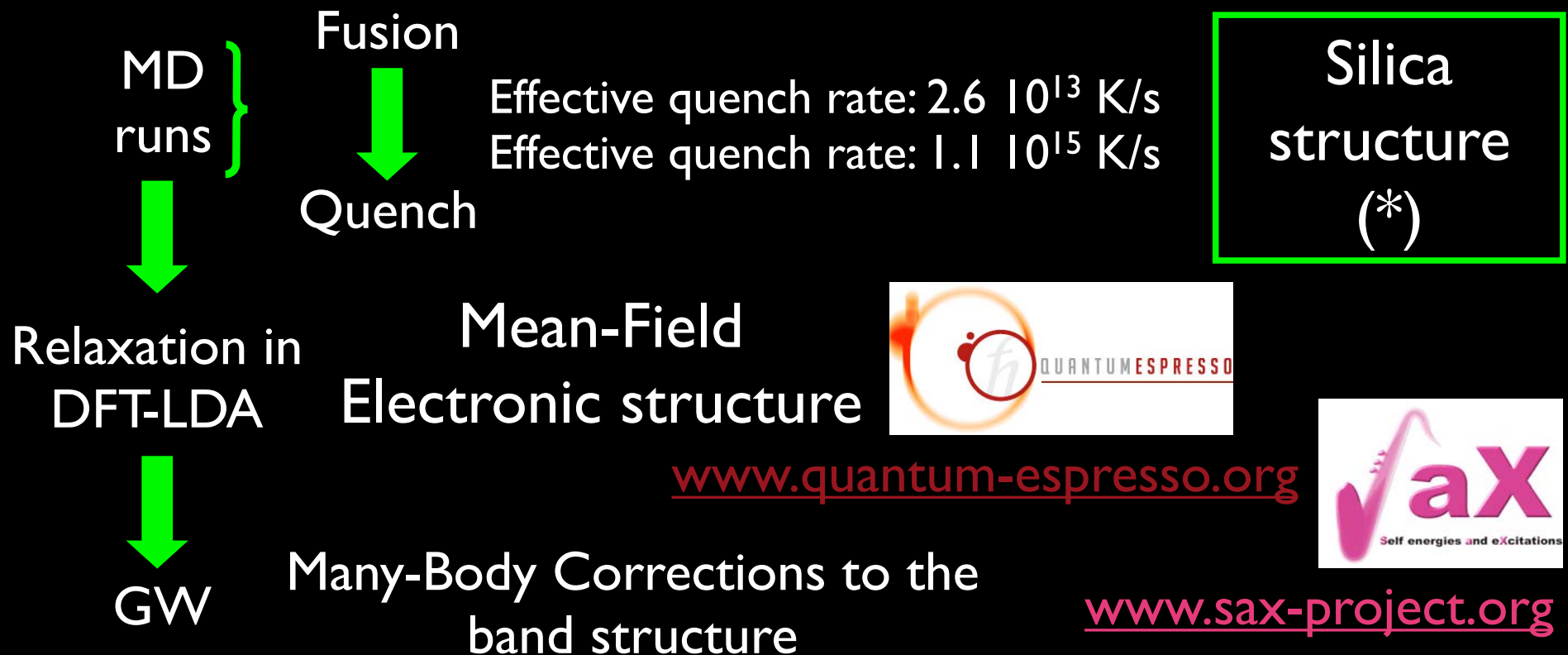
3) L. E. Ramos, J. Furthmuller and F. Bechstedt PRB 69 085102 (2004)

4) E. K. Chang, M. Rohlfing and S. Louie PRL 85 2613 (2000)

Approach

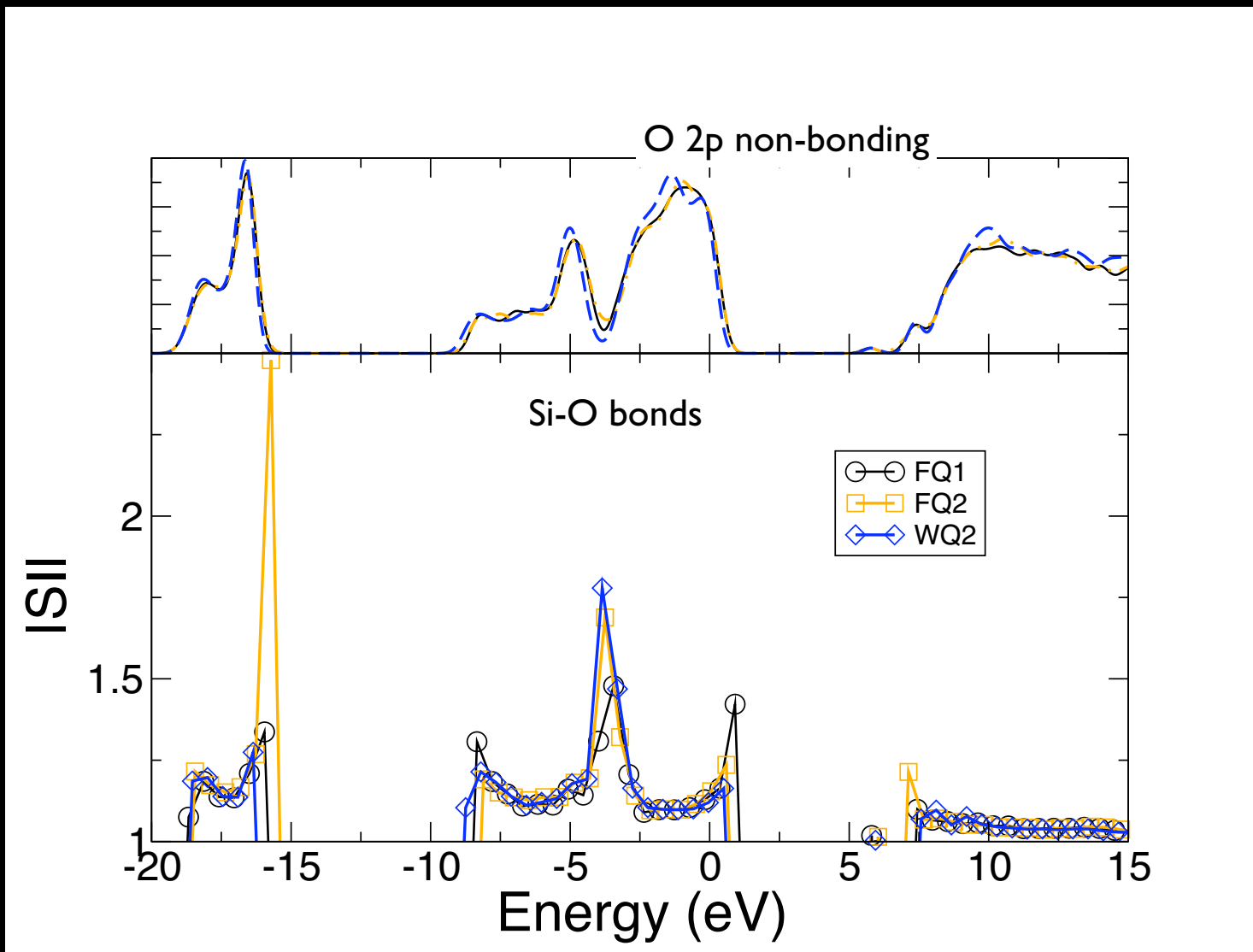
108 atoms silica glass models

Crystal ref. : 108 atoms α -quartz + 24 atoms/192 atoms cristobalite



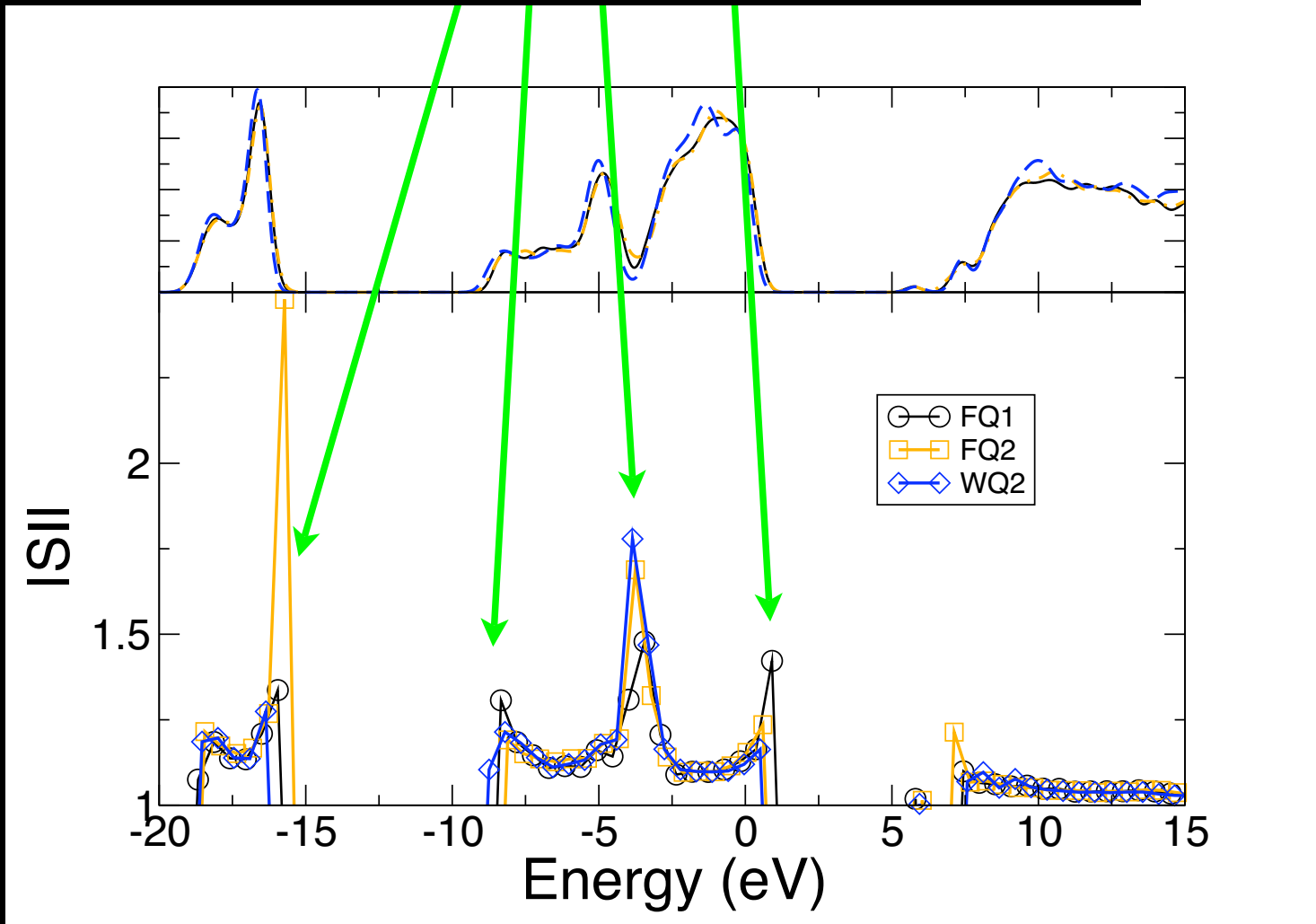
(*) L. Martin-Samos, Y. Limoge, J.P. Crocombette, G. Roma, N. Richard, E. Anglada, E. Artacho, Phys. Rev. B 71 014116 (2005)

Localized tails: quench rate effects



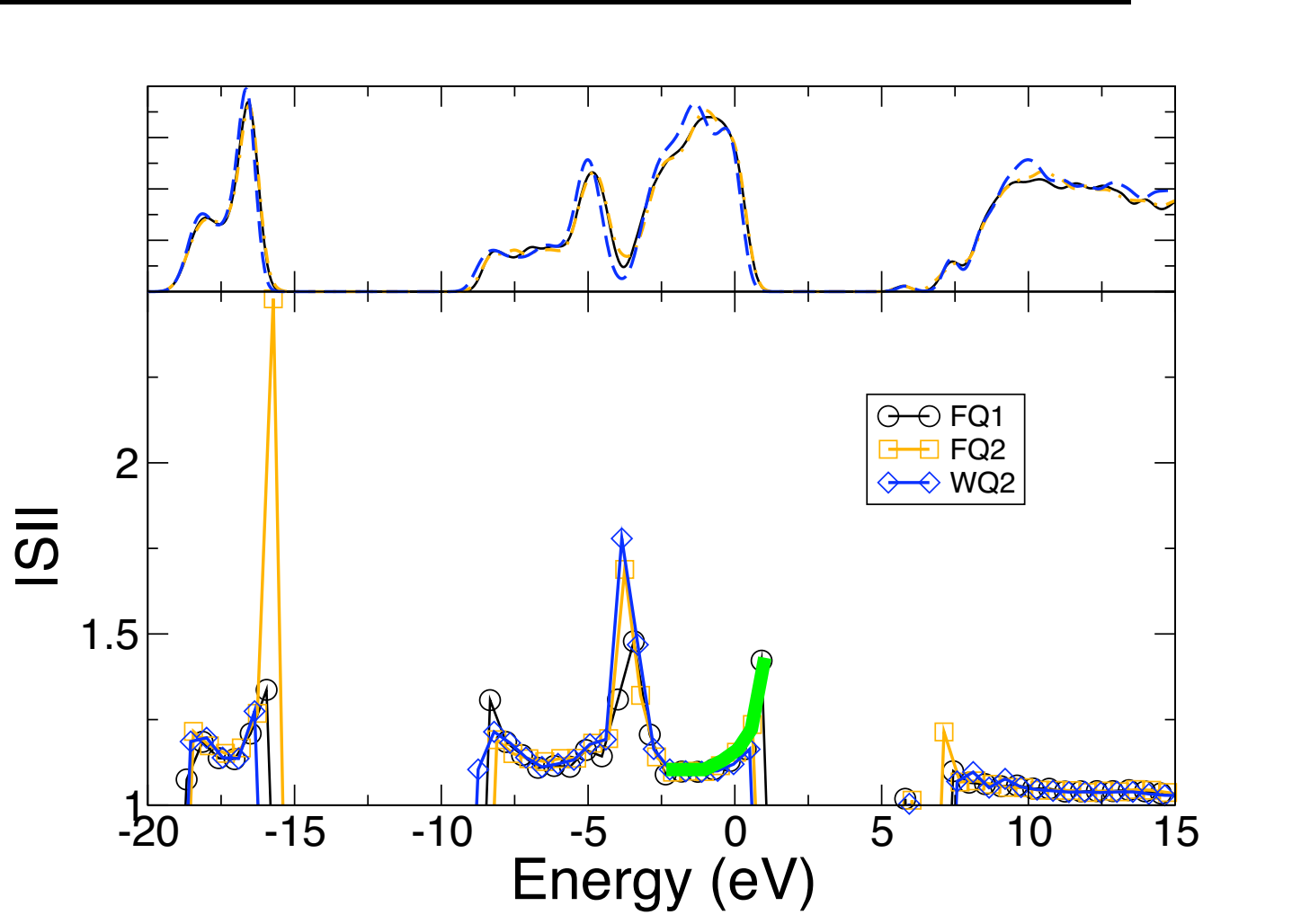
Localized tails: quench rate effects

Signature of localization at valence edges



Localized tails: quench rate effects

The mobility edge is hill defined



Disorder degree and density

	Density	LDA	GW	HF	COHSEX
Cristobalite 0K	2.20	5.4	8.9	-	-
Cristobalite 300 K		5.3	-	-	-
quartz	2.65	5.9	9.4	16.9	10.1
WQ1	2.18	5.6	9.3	16.2	10.1
WQ2	2.27	5.6	9.3		-

Disorder degree and density

	Density	LDA	GW	HF	COHSEX
Cristobalite 0K	2.20	5.4	8.9	-	-
Cristobalite 300 K		5.3	-	-	-
quartz	2.65	5.9	9.4	16.9	10.1
WQ1	2.18	5.6			
WQ2	2.27	5.6			

The gap increases with density

Disorder degree and density

	Density	LDA	GW	HF	COHSEX
Cristobalite 0K	2.20	5.4	8.9	-	-
Cristobalite 300 K		5.3	-	-	-
quartz	2.65	5.9	9.4	16.9	10.1
WQ1	2.18	5.6			
WQ2	2.27	5.6			

Low disorder degree reduces slightly the gap

Disorder degree and density

	Density	LDA	GW	HF	COHSEX
Cristobalite 0K	2.20	5.4	8.9	-	-
Cristobalite 300 K		5.3	-	-	-
quartz	2.65	5.9			
WQ1	2.18	5.6			
WQ2	2.27	5.6			

Strong disorder degree
produces a widening of the
mobility gap

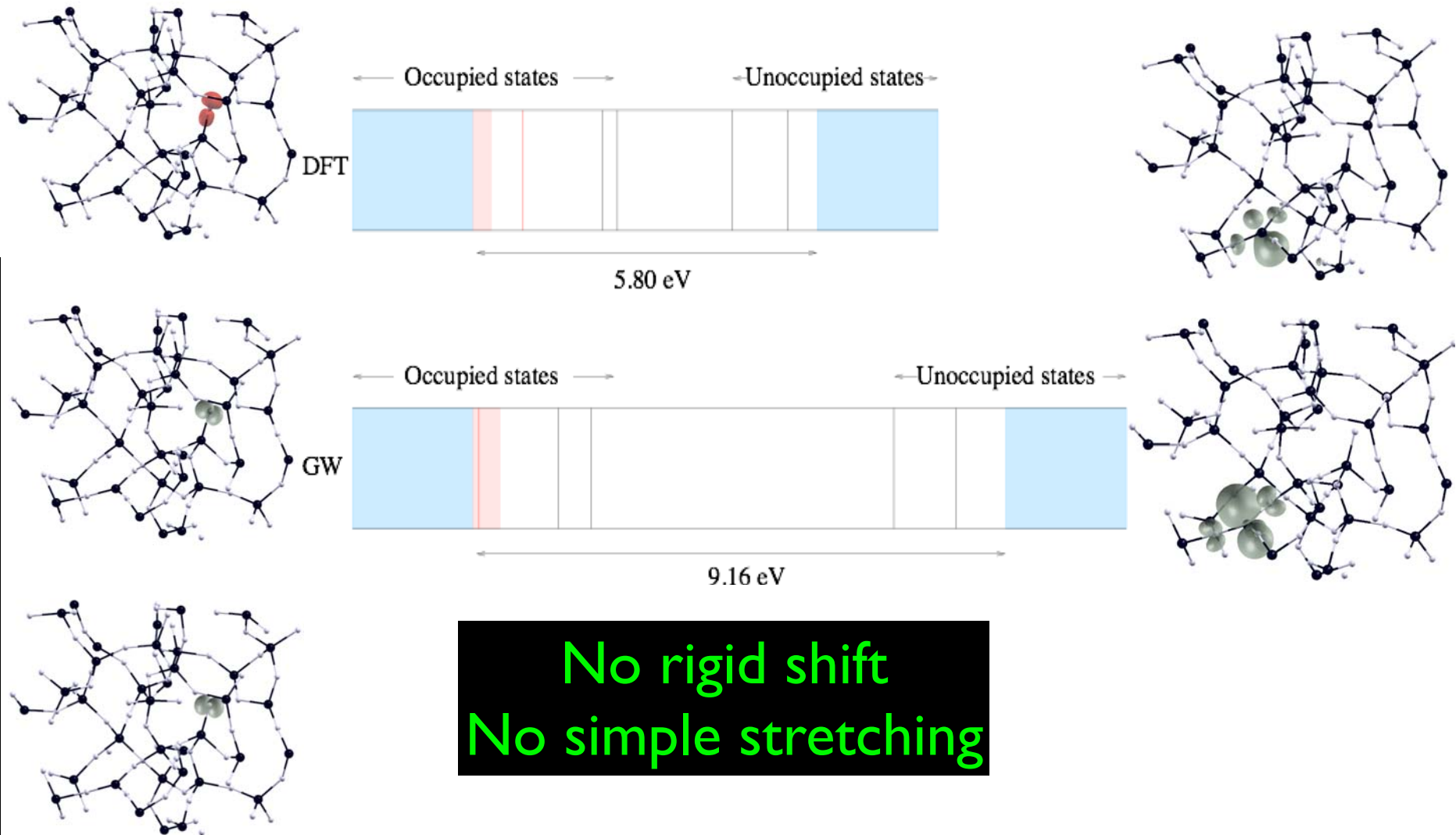
Disorder degree and density

	Density	LDA	GW	HF	COHSEX
Cristobalite 0K	2.20	5.4	8.9	-	-
Cristobalite 300 K		5.3	-	-	-
quartz	2.65	5.9	9.4	16.9	10.1
WQ1	2.18	5.6	9.3	16.2	10.1
WQ2	2.27	5.6	9.3		-

Disorder degree and density

	Density	LDA	GW	HF	COHSEX
Cristobalite 0K	2.20	5.4	8.9	-	-
Cristobalite 300 K		5.3	-	-	-
quartz	2.65	5.9	9.4	16.9	10.1
WQ1	2.18	5.6	9.3	16.2	10.1
WQ2	2.27	5.6	9.3		-

Defects?



Summary

- GW is, at the moment, the best alternative. However, we are now constructing the benchmarks -> recipe? GWs!!!
- Its ingredients are known, to improve it we know the direction to go, contrary to ad-hoc functionals.
- It has been proved that it is strongly transferable.
- Combined with Bethe-Salpeter equation it gives impressive agreement with photo-absorption experiments

2-particle excitations

Coherent linear superposition of vertical single-pair excitations

$$|E\rangle = \sum_{nn'k} A_{nn'k} \hat{a}_{nk}^\dagger \hat{a}_{n'k} |0\rangle + |C\rangle$$

$$\hat{H}|E\rangle = \Omega|E\rangle$$

Higher orders

Only the linear part:

$$\Psi(xx') = \sum_{nn'k} \psi_{nk}^{qp}(x) \psi_{n'k}^{qp*}(x')$$

Effective 2-particle Hamiltonian?

2-particle Green-function and the polarization propagator

Creation

$$G_2(x_1t_1, x_2t_2, x_3t_3, x_4t_4) = (-i)^2 \langle N|T \left[\boxed{\Psi(x_1t_1)\Psi(x_2t_2)} \boxed{\Psi^\dagger(x_3t_3)\Psi^\dagger(x_4t_4)} \right] |N\rangle$$

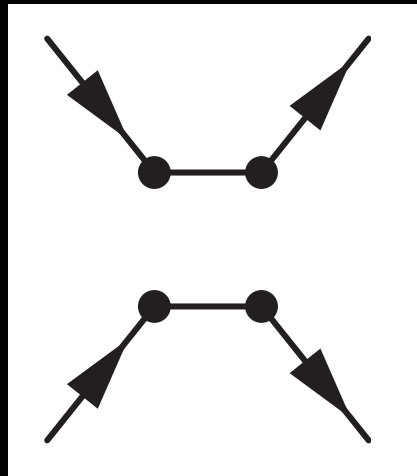
Destruction

$$i\Pi(xt, x't') = \langle N|T \left[\Psi^\dagger(xt^+)\Psi(xt)\Psi^\dagger(x't'^+)\Psi(x't') \right] |N\rangle$$

Lehman representation

$$\Pi_{\lambda\mu,\alpha\beta}(\omega) = \sum_n \left(\frac{\langle N|c_\mu^\dagger c_\lambda|\Psi_n\rangle \langle \Psi_n|c_\alpha^\dagger c_\beta|N\rangle}{\omega - (E_n - E_0) + i\eta} - \frac{\langle N|c_\alpha^\dagger c_\beta|\Psi_n\rangle \langle \Psi_n|c_\mu^\dagger c_\lambda|N\rangle}{\omega - (E_n - E_0) - i\eta} \right)$$

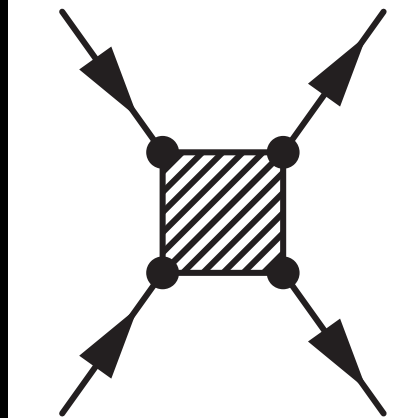
4-point polarizability



$$P^0(1, 1'; 2, 2') = -iG(1', 2')G(2, 1)$$

$$P(1, 1', 2, 2') = P^0(1, 1', 2, 2') +$$

$$+ \int P^0(1, 1', 3, 3')W(3, 3', 4, 4')P(4, 4', 2, 2')d3d3'd4d4'$$



4-point polarizability

Quasi-particle state basis:

$$S(x_1, x_{1'}, x_2, x_{2'}) = \sum_{(n_1, n_{1'})(n_2, n_{2'})} \psi_{n_1}^*(x_1) \psi_{n_{1'}}(x_{1'}) \psi_{n_2}(x_2) \phi_{n_{2'}}^*(x_{2'}) S_{(n_1, n_{1'})(n_2, n_{2'})}$$

Dyson equation

$$\bar{P}_{(n_1, n_{1'})(n_2, n_{2'})} = \bar{P}_{(n_1, n_{2'})(n_2, n_{2'})}^0 + \bar{P}_{(n_1, n_{1'})(n_3, n_{3'})}^0 \Xi_{(n_3, n_{3'})(n_4, n_{4'})} \bar{P}_{(n_4, n_{4'})(n_2, n_{2'})}$$

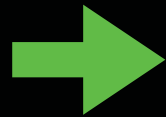
Modified polarizability (reducible)

$$\begin{aligned} \Xi_{(n_1, n_{1'})(n_2, n_{2'})} = & \\ & - \int dx_1 dx_{1'} \psi_{n_1}(x_1) \psi_{n_{1'}}^*(x_{1'}) W(x_1, x_{1'}) \psi_{n_2}^*(x_1) \psi_{n_{2'}}(x_{1'}) + \\ & + \int dx_1 dx_{1'} \psi_{n_1}(x_1) \psi_{n_{1'}}^*(x_1) v(x_1, x_{1'}) \psi_{n_2}^*(x_{1'}) \psi_{n_{2'}}(x_{1'}) \end{aligned}$$

The Bethe-Salpeter Equation

$$((\bar{P}^0)^{-1} - \Xi)P = 1$$

H^{2p}



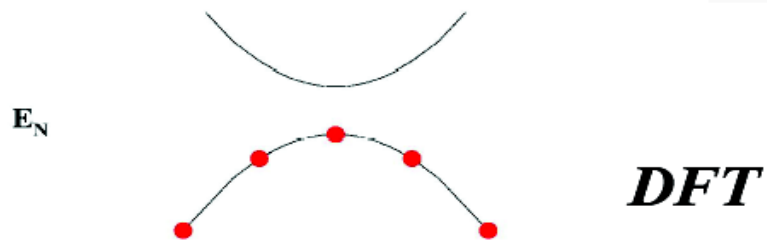
Equivalent eigenvalue equation

$$\sum_{(n_1, n_{1'}) (n_2, n_{2'})} H^{2p}_{(n_1, n_{1'}) (n_2, n_{2'})} A_{(n_2, n_{2'})}^\mu = E^\mu A_{(n_1, n_{1'})}^\mu$$

Effective 2-particle Hamiltonian:

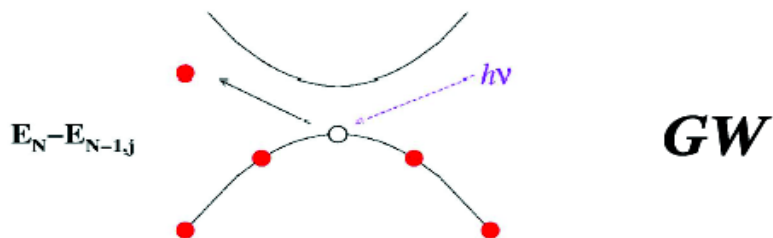
$$H^{2p}_{(n_1, n_{1'}) (n_2, n_{2'})} = (\epsilon_{n_{1'}} - \epsilon_{n_1}) \delta_{(n_1, n_2) (n_{1'}, n_{2'})} + (f_{n_1} - f_{n_{1'}}) \Xi_{(n_1, n_{1'}) (n_2, n_{2'})}$$

Ground State properties (Total energy):



$$\left(-\frac{1}{2}\nabla^2 + V^{ext} + V^H + V_{xc}\right)\phi_j^{KS}(\vec{r}) = \varepsilon_j^{KS}\phi_j^{KS}(\vec{r})$$

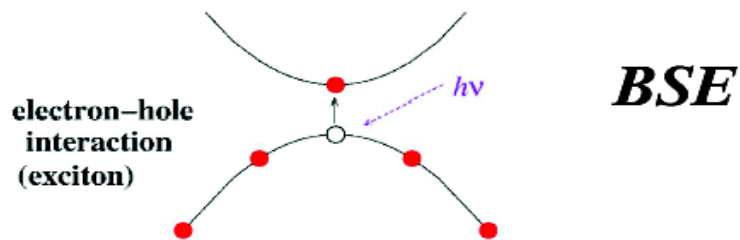
1 particle excitations (photoemission)



$$\left(-\frac{1}{2}\nabla^2 + V^{ext} + V^H\right)\Psi_j^{QP}(\vec{r}) + \int \Sigma(\vec{r}, \vec{r}', \varepsilon_j^{QP})\Psi_j^{QP}(\vec{r}')d\vec{r}' = \varepsilon_j^{QP}\Psi_j^{QP}(\vec{r})$$

$\Sigma = iGW$

2 particle excitations (absorption)

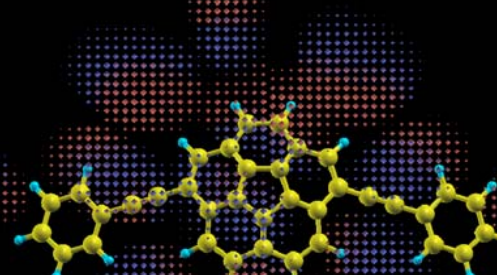
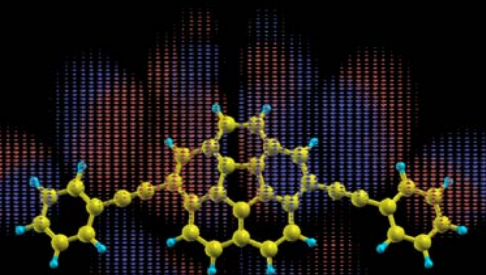
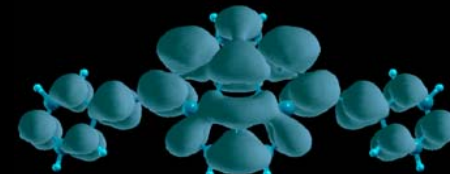
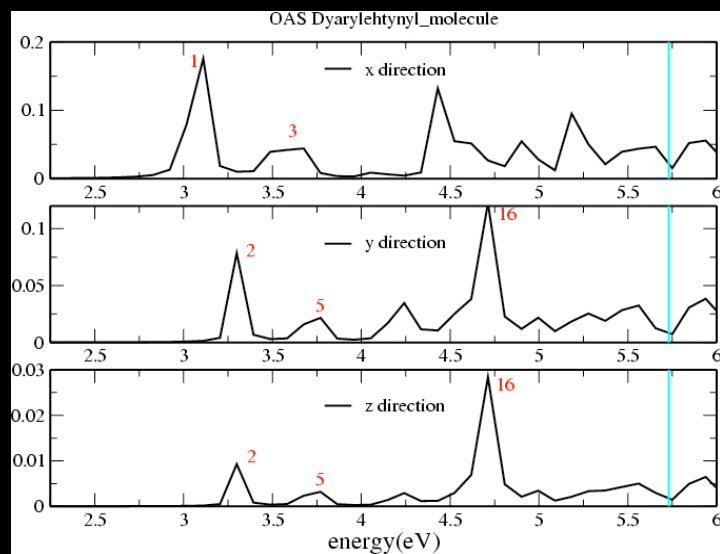


Substituted Corannulene molecule

Transition n.1: 85% HOMO-LUMO

homo DFT

lumo DFT

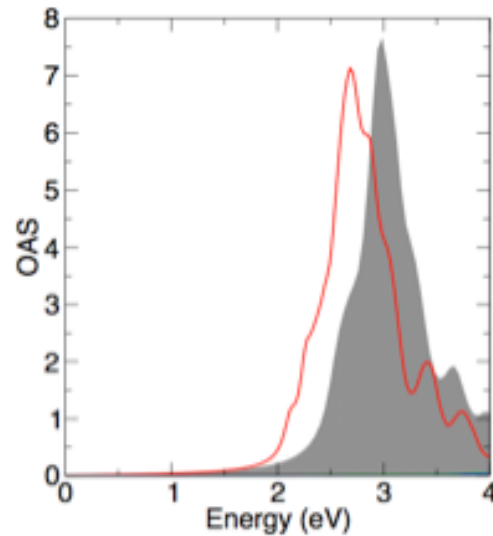


hole

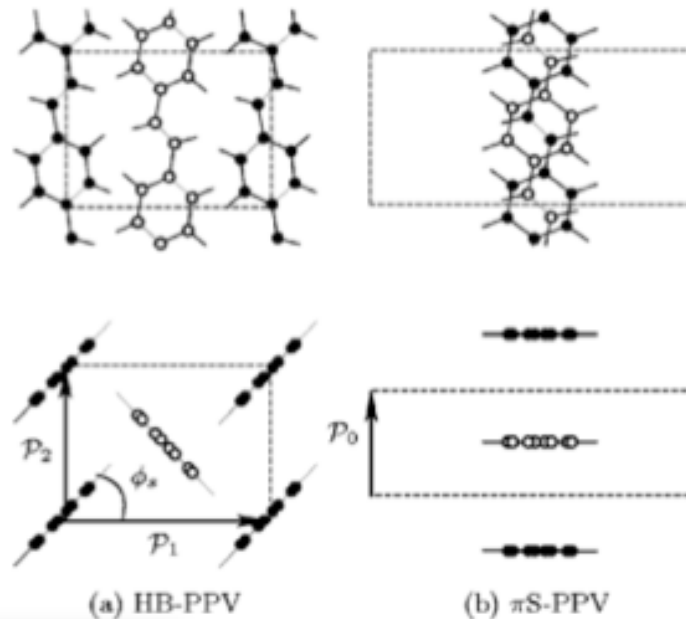
electron

ElectroLuminescent Efficiency in polymers based Light Emitting Diodes

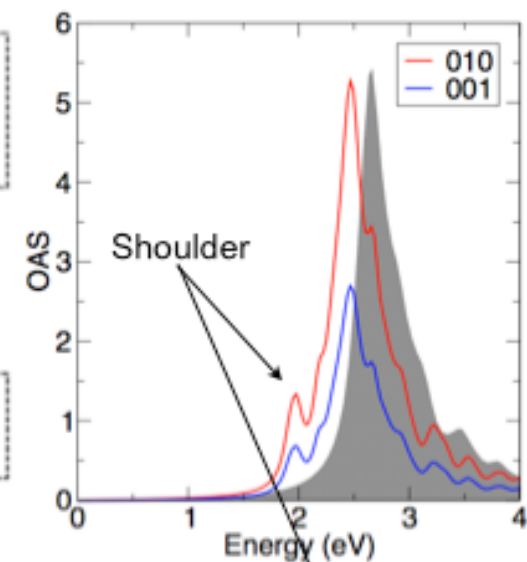
PPV as prototype polymer



Calculated optical absorption spectrum at 0K for HB-PPV

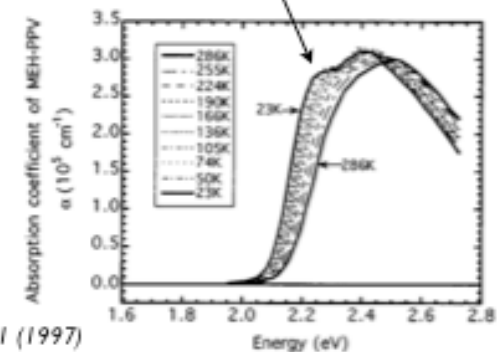


Calculated optical absorption spectrum at 0K for piS-PPV



Converged calculations: 8*runs of 48 hours, 192 procs of HLRB II (LRZ Munich, Germany)

Experimental optical absorption spectrum at different temperatures



Thank you!